Influence of the magnetic field of stellar wind on hot jupiter's envelopes

Dmitry V. Bisikalo and Andrey G. Zhilkin[iD]

Institute of Astronomy of the RAS, 48 Pyatnitskaya str., Moscow, Russia
email: bisikalo@inasan.ru

Abstract. Hot Jupiters have extended gaseous (ionospheric) envelopes, which extend far beyond the Roche lobe. The envelopes are loosely bound to the planet and, therefore, are strongly influenced by fluctuations of the stellar wind. We show that, since hot Jupiters are close to the parent stars, magnetic field of the stellar wind is an important factor defining the structure of their magnetospheres. For a typical hot Jupiter, velocity of the stellar wind plasma flow around the atmosphere is close to the Alfvén velocity. As a result stellar wind fluctuations, such as coronal mass ejections, can affect the conditions for the formation of a bow shock around a hot Jupiter. This effect can affect observational manifestations of hot Jupiters.

Keywords. MHD, stars: winds, stars: planetary systems

1. Introduction

Hot Jupiters are exoplanets which have mass of the same order as Jupiter and are located in the close proximity to the parent star (Murray-Clay *et al.* (2009)). The first hot Jupiter was discovered in 1995 (Mayor & Queloz (1995)). Due to their proximity to the parent star and relatively large dimensions of the envelopes hot Jupiters can overflow the Roche lobes. This leads to the outflows from the vicinity of the nearest Lagrange points (Li *et al.* (2010); Bisikalo *et al.* (2013)). This circumstance is indirectly indicated by the the excess absorption in the near UV, observed for some planets of this type (Vidal-Madjar *et al.* (2003, 2008); Ben-Jaffel (2007); Vidal-Madjar *et al.* (2004); Ben-Jaffel & Sona Hosseini (2010); Linsky *et al.* (2010)). Therefore, the study of the mechanisms of mass loss by hot Jupiters is one of the most urgent tasks of modern astrophysics.

The structure of the gaseous envelopes of hot Jupiters was investigated in a series of our studies, using three-dimensional numerical models (see. e.g.. (Bisikalo *et al.* (2013); Cherenkov *et al.* (2014); Bisikalo & Cherenkov (2016); Cherenkov *et al.* (2017, 2018); Bisikalo *et al.* (2018)). It is shown that gaseous envelopes of three main types may form around hot Jupiters, depending on the model parameters. In the case of close envelope, planet's atmosphere is completely located inside its Roche lobe. Open envelope is formed by outflows from the nearest Lagrange points. If dynamic pressure of the stellar wind stops the outflow beyond Roche lobe, quasi-closed envelope is formed. The rate of mass-loss substantially depends on the type of the gaseous envelope being formed.

Arakcheev *et al.* (2017), Bisikalo *et al.* (2017) presented results of the three-dimensional numerical simulation of the flow structure in the vicinity of a hot Jupiter WASP 12b that took into account the influence of the planet's proper magnetic field. Computations have shown that the presence of the planet's magnetic field can lead to the additional decline of the mass-loss rate compared to the purely gas-dynamic case. The analysis by Zhilkin & Bisikalo (2019) has shown that a very important factor is magnetic field of the stellar

wind, since many hot Jupiters are located in the sub-Alfvén zone of the stellar wind, where magnetic pressure exceeds dynamic one. In this case, the flow can be shockless (Ip *et al.* (2004)).

Various perturbations of the stellar wind can lead to significant changes in the structure of the gaseous envelopes of hot Jupiters and, consequently, to the variations of the mass-loss rate. The most significant wind disturbances (coronal mass ejections, henceforth, CME) arise due to giant ejections of matter from the stellar corona. Bisikalo & Cherenkov (2016), Cherenkov *et al.* (2017), using three-dimensional numerical simulations, have shown that even in the case of a typical solar-like CME external parts of the asymmetric gaseous envelope of a hot Jupiter that are outside Roche lobe can be torn and carried away into the interplanetary medium. This leads to a sharp increase in the rate of mass loss by a hot Jupiter at the moment, when CME passes it.

In the present paper, we study the effect of stellar wind magnetic field on the structure of the ionospheric envelopes of hot Jupiters. In particular, we consider some interesting features of the interaction of a CME with the magnetosphere of a hot Jupiter due to the variation of the parameters of magnetic field of stellar wind. The paper is based on our recent studies (Zhilkin & Bisikalo (2019); Zhilkin, Bisikalo & Kaygorodov (2020)).

2. MHD model of stellar wind

To describe stellar wind in the vicinity of hot Jupiters in our numerical model, we will rely on the well-studied properties of the solar wind. As it is shown by numerous Earth-based and space studies (see, for instance, recent review by Owens & Forsyth (2013)), solar wind magnetic field has a rather complex structure. In the corona region, magnetic field structure is defined mainly, by the intrinsic magnetism of the Sun and, therefore, it is essentially non-radial. At the border of the corona, which is at a distance of several solar radii, magnetic field to a large accuracy becomes completely radial. Outside this region, the heliospheric region is located, where magnetic field is largely determined by the properties of the solar wind. In the heliospheric region, magnetic field lines, as they gradually recede from the center, twist into a spiral due to the solar rotation and, therefore (especially at large distances), magnetic field of the wind with a good accuracy can be described using the simple Parker (1958) model.

In our calculations, we do not take into account possible sectoral structure of the magnetic field of the wind, focusing on the account of the influence of its global parameters. We assume that the orbit of the hot Jupiter is located in the heliospheric region beyond the border of the corona. To describe the structure of the wind (including its magnetic field **B**) in the heliospheric region, as the first approximation, one can apply axisymmetric magnetohydrodynamic model (Weber & Davis (1967)). The model of the wind will be considered in the inertial reference frame in spherical coordinates (r, θ, φ). One can neglect the dependence of wind parameters on the angle θ, because we are interested in the flow structure close to the orbital plane. Therefore, we will assume that all quantities depend on the radial coordinate r only.

Under such assumptions, steady-state structure of the wind is defined by the continuity equation

$$\frac{1}{r^2}\frac{d}{dr}\left(r^2 \rho v_r\right) = 0, \tag{2.1}$$

equations of motion for radial v_r and azimuthal v_φ components of the velocity vector **v**

$$v_r \frac{dv_r}{dr} - \frac{v_\varphi^2}{r} = -\frac{1}{\rho}\frac{dP}{dr} - \frac{GM}{r^2} - \frac{B_\varphi}{4\pi\rho r}\frac{d}{dr}\left(r B_\varphi\right), \tag{2.2}$$

$$v_r \frac{dv_\varphi}{dr} + \frac{v_r v_\varphi}{r} = \frac{B_r}{4\pi\rho r} \frac{d}{dr} \left(r B_\varphi \right), \tag{2.3}$$

induction equation

$$\frac{1}{r} \frac{d}{dr} \left(r v_r B_\varphi - r v_\varphi B_r \right) = 0 \tag{2.4}$$

and Maxwell equation $(\nabla \cdot \mathbf{B} = 0)$

$$\frac{1}{r^2} \frac{d}{dr} \left(r^2 B_r \right) = 0. \tag{2.5}$$

Here, ρ is density, P — pressure, G — gravity constant, M — mass of the central star. Density, pressure, and temperature satisfy the equation of state for ideal polytropic gas

$$P = P_0 \left(\frac{\rho}{\rho_0} \right)^\gamma = \frac{2k_B}{m_p} \rho T, \tag{2.6}$$

where k_B — Boltzmann constant, m_p — proton mass, γ — polytropic exponent. Mean molecular weight of the wind matter is assumed to be 0.5, corresponding to the completely ionized hydrogen plasma containing electrons and protons only. Index 0 defines the quantities in point r_0.

From Maxwell equation (2.7) we obtain

$$B_r = B_s \left(R_s / r \right)^2, \tag{2.7}$$

where R_s is stellar radius, B_s — the field strength at the stellar surface. From continuity equation (2.1) it is possible to derive the integral of motion, corresponding to the mass conservation law:

$$r^2 \rho v_r = \text{const.} \tag{2.8}$$

Equation (2.2) allows to derive the motion integral, corresponding to the energy conservation law:

$$\frac{v_r^2}{2} + \frac{v_\varphi^2}{2} + \frac{c_s^2}{\gamma - 1} - \frac{GM}{r} - \frac{B_\varphi^2}{4\pi\rho} - \frac{B_r B_\varphi v_\varphi}{4\pi\rho v_r} = \text{const}, \tag{2.9}$$

where sound velocity

$$c_s = \sqrt{\gamma P / \rho}. \tag{2.10}$$

Note, it follows from Eqs. (2.7) and (2.8) that

$$\frac{B_r}{4\pi\rho v_r} = \text{const.} \tag{2.11}$$

This circumstance allows to derive from Eqs. (2.3) and (2.4) two integrals of motion more:

$$r v_\varphi - \frac{B_r}{4\pi\rho v_r} r B_\varphi = L, \tag{2.12}$$

$$r v_r B_\varphi - r v_\varphi B_r = F. \tag{2.13}$$

The value of the constant F in the motion integral (2.13) could be found from the boundary conditions at the stellar surface at $r = R_s$:

$$B_\varphi = 0, \quad B_r = B_s, \quad v_\varphi = \Omega_s R_s, \tag{2.14}$$

where Ω_s is angular velocity of the proper stellar rotation. Therefore,

$$F = -\Omega_s R_s^2 B_s = -\Omega_s r^2 B_r. \tag{2.15}$$

This integral can also be interpreted in the sense that in the reference frame of the rotating star velocity vector **v** of the perfectly conducting wind plasma must be collinear to the magnetic field induction vector **B**. With account of this expression, solutions of the Eqs. (2.12) and (2.13) can be written as:

$$v_\varphi = \frac{\Omega_s r - \lambda^2 L/r}{1 - \lambda^2}, \tag{2.16}$$

$$B_\varphi = \frac{B_r}{v_r} \lambda^2 \frac{\Omega_s r - L/r}{1 - \lambda^2}. \tag{2.17}$$

Here, as λ we denote Alfvén Mach number for radial components of velocity and magnetic field,

$$\lambda = \frac{\sqrt{4\pi\rho}\, v_r}{B_r}. \tag{2.18}$$

Close to the surface of a star, radial wind velocity v_r should be lower than Alfvén velocity $u_A = B_r/\sqrt{4\pi\rho}$ and the parameter $\lambda < 1$. On the contrary, at large distances, radial velocity v_r, exceeds Alfvén velocity u_A ($\lambda > 1$). This means that at some distance from the stellar center $r = r_A$ (Alfvén point) the parameter λ becomes equal to 1. The region $r < r_A$ can be named *sub-Alfvén* zone of the stellar wind, while the region $r > r_A$, accordingly, *super-Alfvén* zone.

The values of v_φ and B_φ in the Eqs. (2.16) and (2.17) should be continuous in the Alfvén point $r = r_A$. Therefore, it is necessary to set

$$L = \Omega_s r_A^2. \tag{2.19}$$

As a result, we find the final solution

$$v_\varphi = \Omega_s r \frac{1 - \lambda^2 r_A^2/r^2}{1 - \lambda^2}, \tag{2.20}$$

$$B_\varphi = \frac{B_r}{v_r} \Omega_s r \lambda^2 \frac{1 - r_A^2/r^2}{1 - \lambda^2}. \tag{2.21}$$

These relations, with the integrals of mass (2.8) and energy (2.9) taken into account, allow, using algebra, to obtain the distributions of all magnetohydrodynamic quantities describing the structure of the wind. At this, to single out a unique solution, it is necessary to use continuity conditions in three critical points at which the radial wind velocity v_r is equal, respectively, to slow magneto-sonic

$$u_S = \left\{ \frac{1}{2} \left[c_s^2 + a^2 - \sqrt{(c_s^2 + a^2)^2 - 4c_s^2 u_A^2} \right] \right\}^{1/2}, \tag{2.22}$$

Alfvén u_A, and fast magneto-sonic

$$u_F = \left\{ \frac{1}{2} \left[c_s^2 + a^2 + \sqrt{(c_s^2 + a^2)^2 - 4c_s^2 u_A^2} \right] \right\}^{1/2}, \tag{2.23}$$

velocities. Here,

$$a^2 = \frac{B_r^2 + B_\varphi^2}{4\pi\rho}. \tag{2.24}$$

It is interesting to note that solutions with accelerating wind (positive value of the radial velocity gradient, $dv_r/dr > 0$) are realized for polytropic exponent $\gamma < 3/2$ only. This indicates the presence of effective sources of heating and cooling. It is known that the solar wind at small distances from the Sun ($r < 15R_\odot$) turns out to be almost isothermal, since the effective adiabatic exponent $\gamma = 1.1$ (Steinolfson & Hundhausen (1988);

Roussev *et al.* (2003)). At large distances, $r > 25R_\odot$, the effective adiabatic exponent can be estimated as $\gamma = 1.46$ (Totten *et al.* (1995)). As the orbits of hot Jupiters are located close to the parent stars, in the calculations of the wind structure we used adiabatic exponent $\gamma = 1.1$. Model parameters corresponded to the the distance from the star $r_0 = 10R_\odot$, which is typical for the orbits of hot Jupiters. Number density $n_0 = 1400\ \text{cm}^{-3}$ and temperature $T_0 = 7.3 \cdot 10^5$ K were chosen (Withbroe (1988)). Corresponding resulting distributions were used in our numerical models for description of the magnetohydrodynamic structure of stellar wind in the neighborhood of hot Jupiter. In particular, radial wind velocity at the distance $r_0 = 10R_\odot$ from the star turned out to be of the order of $v_{r,0} = 130$ km/s.

3. Magnetspheres of hot jupiters

In the solar wind, Alfvén radius $r_A = 0.11$ AU $= 24.3R_\odot$ (Weber & Davis (1967)). Since the semi-major axis of the orbit of the innermost planet, Mercury, is 0.38 AU $= 82R_\odot$, this means that all planets of the solar system are in the super-Alfvén zone of the solar wind. Sonic point, where wind velocity becomes comparable to the sound speed in the solar wind is even closer to the Sun, at a distance of approximately 0.037 AU $= 8R_\odot$. It follows then, that the magnetospheres of all planets in the solar system (if they have them) have similar structure, like that of the terrestrial magnetosphere. They are characterized by the following set of basic elements: bow shock, transition region, magnetopause, radiation belts, magnetospheric tail.

In the case of hot Jupiters, due to their proximity to the parent star, the structure of magnetospheres may be completely different. To analyze possible configurations, we processed actual data for a sample of 210 hot Jupiters from the database at www.exoplanet.eu. Selection was carried out according to the masses of the planets ($M_p > 0.5M_\text{jup}$, where M_jup is the mass of Jupiter), orbital period ($P_\text{orb} < 10$ day), and semi-major axis of the orbit ($A < 10R_\odot$). Additionally, only planets for which all necessary data were known were left in the sample.

As the model of stellar wind in the immediate vicinity of the Sun, at the distances $1R_\odot < r < 10R_\odot$, we applied the results of computations by Withbroe (1988). According to the obtained profiles of density $\rho(r)$ and radial velocity $v_r(r)$, for each hot Jupiter in the sample dynamic wind pressure at the orbit of the planet

$$P_\text{dyn} = \rho(A)v_r^2(A) \tag{3.1}$$

and magnetic pressure

$$P_\text{mag} = \frac{B_r^2(A)}{8\pi} \tag{3.2}$$

were calculated. The radial field value was computed by the formula $B_r(A) = B_\text{s}(R_\odot/A)^2$ with the parameter $B_\text{s} = 1$ G. Thus obtained distribution of hot Jupiters in the two-dimensional diagram P_mag–P_dyn is presented in the left panel of Fig. 1. Positions of the planets correspond to the centers of the circles with radii determined by the mass M_p (in the logarithmic scale). Solid line shows position of the Alfvén point of the solar wind, which corresponds to a simple relation $P_\text{dyn} = 2P_\text{mag}$.

As can be seen from the obtained distribution, all hot Jupiters from this sample are located in the sub-Alfvén zone of the stellar wind. However, in the reference frame, associated with an orbiting planet, the nature of the flow is determined not only by the wind velocity, but also by the orbital velocity of the planet. If this is taken into consideration, dynamic pressure becomes

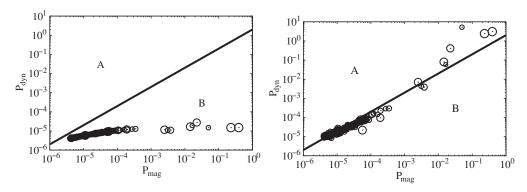$$P_\text{dyn} = \rho(A)\left[v_r^2(A) + \frac{G(M_s + M_p)}{A}\right]. \tag{3.3}$$

Figure 1. Distribution of hot Jupiters in the scattering diagram P_{mag}–P_{dyn}. Alfvén Mach numbers calculated with account of wind velocity only are presented in the left panel; the right panel shows orbital velocities of the planets. Parameters of the planets were taken from the database at www.exoplanet.eu. The data for 210 hot Jupiters were used. Locations of the planets are at the centers of the circles. The sizes of the circles correspond to the masses of the planets in the logarithmic scale. Solid line shows the position of Alfvén point of the solar wind. The letters mark super-Alfvén zone ("A") and sub-Alfvén zone ("B").

Note that the orbital velocity of the planet depends not only on the radius of the orbit, but also on the mass of the planet. The corresponding diagram is shown in the right panel of Fig. 1. Account of the orbital velocity shifts whole sequence significantly up toward the super-Alfvén zone of the wind. Note that most of the planets in this diagram form a regular sequence (lower left corner of the diagram). These planets are located rather far from the star, where the dependences of density and wind velocity on the radius are well described by power laws. Planets that are close to the star are scattered over the diagram rather chaotic. For these planets, the dynamic wind pressure (3.3) is determined mainly by their orbital velocity.

Because for hot Jupiters with orbits located in the sub-Alfvén zone, Alfvén Mach number $\lambda = v_r/u_A$ turns out to be less than one, the ratio v_r/u_F, where u_F is the fast magneto-sonic velocity (2.23) will also be less than one, since, obviously, $u_F > u_A$ and, therefore, the ratio $v_r/u_F < v_r/u_A$. In other words, in the neighborhood of such a hot Jupiter, stellar wind velocity will be lower than the fast magneto-sonic speed. In the pure gas dynamics, this case corresponds to the subsonic flow around the body, in which the bow shock does not form. Thus, we come to the following conclusion: the flow of stellar wind around such a hot Jupiter should be shockless (Ip *et al.* (2004)). In the structure of the magnetosphere of hot Jupiter, the bow shock should be absent.

It should be borne in mind that this distribution was obtained for the solar wind in the model of a quite Sun. At this, we assumed that the average value of the magnetic field at the surface of the Sun is 1 G. Even for the Sun, during its activity cycle, the position of hot Jupiters in the right panel of Fig. 1 can change respective to the Alfvén point in both directions. In reality, each planet in our sample is flown around not by the solar wind, but by the stellar wind of the parent star. The parameters of this wind may differ significantly from the solar one. This means that the mode of the flow of stellar wind around the atmosphere of the planet must be investigated separately in every specific case, taking into account individual characteristics of the planet and the parent star.

Let treat as the ionospheric envelope the upper layers of the atmosphere of a hot Jupiter, which are composed by almost completely ionized gas (Cherenkov *et al.* (2018)). A closed ionospheric envelope corresponds to the case when the atmosphere of a hot Jupiter is entirely located inside its Roche lobe. An open ionospheric envelope corresponds to the case when hot Jupiter overflows its Roche lobe, forming outflows from the vicinity
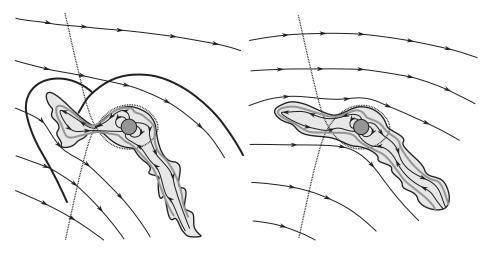
Figure 2. A sketch of the structure of an impact-induced magnetosphere (left panel) and shockless induced magnetosphere (right panel) for the case of open ionospheric envelope of a hot Jupiter. The lines with arrows correspond to the magnetic field lines. Dashed line shows the Roche lobe border. Light-gray region corresponds to the gaseous envelope of the star. Solid outer line shows location of the shock. Position of magnetopause is shown by inner gray line.

of the Lagrange points L_1 and L_2. Since proper magnetic field of hot Jupiters is rather weak, the magnetopause is located inside the ionospheric envelope. In such a situation, the most likely types of magnetospheres of hot Jupiters are an impact induced magnetosphere (see the left panel in Fig. 2) and a shockless induced magnetosphere (see the right panel in Fig. 2).

An induced magnetosphere (Russell (1993)) is formed by the currents that are excited in the upper layers of the ionosphere. These currents partially shield the magnetic field of the wind. As a result, magnetic lines of the the generated field enshroud the ionosphere of the planet, forming a peculiar magnetic barrier or ionopause. Bow shock wave sets immediately in the front of this barrier. On the night side a magnetospheric tail is formed, which can be partially filled by the plasma from the ionosphere. At difference to proper magnetosphere (similar to that of the Earth or the Jupiter), orientation of the magnetic field in the induced magnetosphere is completely determined by the field of the wind. As the result, when the planet moves in its orbit, entire structure of the magnetosphere tracks direction to the star. In the solar system, this situation for the case of a closed ionospheric envelope corresponds to the magnetosphere of the Venus and, in some sense, to that of the Mars. Induced magnetospheres with open ionospheric envelopes can form in the comets coming close to the Sun.

A curious situation may arise in the intermediate case (a "gray" zone), when the orbit of a hot Jupiter is close to the Alfvén point. In particular, in this case the planet itself may be located in sub- or super-Alfvén zone of the wind, while the outflowing ionospheric envelope, due to its rather large extent, can cross the Alfvén point and partially flow into the opposite wind zone. For hot Jupiters this case may turn out to be quite common, because the overwhelming majority of them are located just close to the Alfvén point.

4. Hot jupiters in sub-alfvenic and super-alfvenic zones

Our analysis allows to conclude that in the vicinity of almost of all currently known hot Jupiters velocity of the stellar wind turns out to be close to the Alfvén velocity. However, many of them can be located even in the sub-Alfvén zone, where magnetic pressure of the stellar wind exceeds its dynamic pressure. This means that for the study
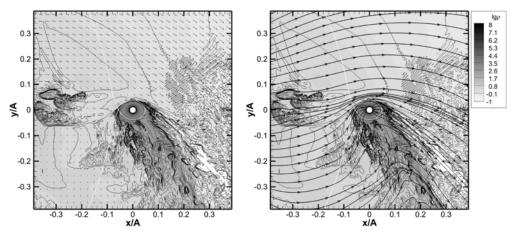
Figure 3. Distributions of the density (gray scale and level lines), velocity and magnetic field (lines with arrows) in the plane of the orbit of a hot Jupiter. Presented is solution for a model with a strong stellar wind field ($B_s = 0.5$ G) at the instant $0.5P_{orb}$ from the reference-starting point. Dashed line shows the boundary of the Roche lobe. The circle corresponds to the photometric radius of the planet.

Figure 4. Distributions of the density (gray scale and level lines), velocity and magnetic field (lines with arrows) in the plane of the orbit of a hot Jupiter. Presented is solution for a model with a weak stellar wind field ($B_s = 0.5$ G) at the instant $0.26P_{orb}$ from the reference-starting point. Dashed line shows the boundary of the Roche lobe. The circle corresponds to the photometric radius of the planet.
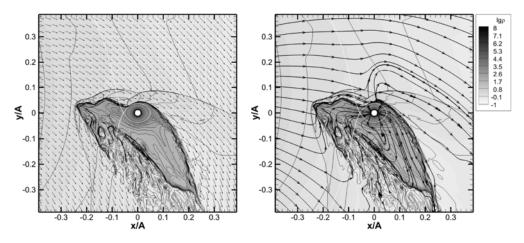
of the stellar wind flow around the ionospheric envelope of a hot Jupiter magnetic field of the wind is an important factor, which is absolutely necessary to take into account both in theoretical modeling and in interpretation of the observational data.

In Figs. 3 and 4 we present results of the three-dimensional numerical simulation of the flow structure in the vicinity of the hot Jupiter HD 209458b (Charbonneau *et al.* (2000)). For calculations, we applied numerical model described by Zhilkin & Bisikalo (2019). The main parameters of the model were the same as in our previous studies (see, e.g., Bisikalo *et al.* (2013)). Spectral type G0 parent star HD 209458 has the mass $M_s = 1.15M_\odot$ and the radius $R_s = 1.2R_\odot$. Proper rotation of the star is characterized by the period $P_{rot} = 14.4$ day, which corresponds to the angular velocity $\Omega_s = 5.05 \cdot 10^{-6}$ s^{-1} or linear velocity at the equator $v_{rot} = 4.2$ km/s. Mass of the planet is $M_p = 0.71M_{jup}$, its

photometric radius is $R_p = 1.38 R_{\rm jup}$, where $R_{\rm jup}$ is the radius of the Jupiter. Semimajor axis of the orbit of the planet $A = 10.2 R_{\odot}$, which corresponds to the period of orbital revolution $P_{\rm orb} = 84.6$ hr.

At the initial moment of time, a spherically symmetric isothermal atmosphere was set around the planet, the density distribution in which was determined from the condition of hydrostatic equilibrium. The radius of the atmosphere was determined from the condition of pressure equilibrium with stellar wind matter. The temperature of the atmosphere was set equal to $T_{\rm atm} = 7500$ K, while number density of the particles at the photometric radius was taken as $n_{\rm atm} = 10^{11}$ cm^{-3}.

As stellar wind parameters were taken the values appropriate for the solar wind at the distance of $10.2 R_{\odot}$ from the center of the Sun (Withbroe (1988)): temperature $T_w = 7.3 \cdot 10^5$ K, velocity $v_w = 100$ km/s, number density $n_w = 10^4$ cm^{-3}. Magnetic field of the wind was set according to the formulas given in Zhilkin & Bisikalo (2019). Calculations were performed for two models, corresponding to the cases of weak and strong magnetic field of stellar wind. The average magnetic field at the surface of the star was set equal to $B_{\rm s} = 0.5$ G for the first model (strong field) and $B_{\rm s} = 0.01$ G for the second model (weak field). Given the fact that the radius of the star is slightly greater than the radius of the Sun, the magnitude of the field in the first model practically corresponds to the average magnetic field at the surface of the Sun, if corresponding magnetic moments of stars are compared.

In the numerical model, we also took into account proper magnetic field of the planet. At this, we assumed that the value of the magnetic moment of the hot Jupiter HD 209458b $\mu = 0.1 \mu_{\rm jup}$, where $\mu_{\rm jup} = 1.53 \cdot 10^{30}$ G $\cdot$ cm^3 is the magnetic moment of the Jupiter. This value is consistent both with observations (Kislyakova et al. (2014)) and with theoretical estimates (Stevenson (1983)). The axis of the magnetic dipole was tilted by 30° to the axis of rotation of the planet, in the direction opposite to the star. It was assumed in the model that rotation of the planet is synchronized with the orbital revolution and the axis of proper rotation is collinear with the axis of orbital rotation.

In the first model (strong field), the sub-Alfvén flow regime is realized. As can be seen from Fig. 3, in this case, the process of interaction of stellar wind with the ionospheric envelope of the planet is shockless. The detached shock wave is formed neither around the planet atmosphere nor around the matter ejected from L_1. This is clearly seen from the density and velocity distributions (see the left panel in Fig. 3). Magnetic field of the wind is so strong that it prevents the free motion of the plasma in the direction transverse to the field lines. Therefore, the ejected matter moves toward the star mainly along the magnetic field lines of the wind (see the right panel in Fig. 3). For that reason, we can say that in this process electromagnetic force, due to the magnetic field of the wind, plays an important role, comparable to the role of stellar gravity, centrifugal force, and Coriolis force.

In the second model (weak field), the super-Alfvén flow regime is realized. As a result of the interaction of the stellar wind with the planet's ionospheric envelope, a detached shock wave forms. This is clearly seen in Fig. 4. It can be stated that this shock wave consists of two separate shock waves, one of which occurs when the wind interacts directly with the atmosphere of the planet, and the other — when it interacts with the matter of the jet from the inner Lagrange point L_1. Inside Roche lobe of the planet magnetic field retains the dipole structure. However, in the flows forming on the day- and night-sides, the lines of the original dipole field are strongly stretched and distorted. Since in this model magnetic field of the stellar wind is weak and does not play any significant dynamic role, flow pattern corresponds to the purely gas-dynamic case described in Bisikalo et al. (2013).

5. Effect of CME on the magnetospheres of hot jupiters

Various perturbations of the stellar wind, such as, for instance, CMEs, can lead to to the significant changes in the structure of the gaseous envelopes of hot Jupiters and, therefore, to variations in the rate of mass loss. Even in the case of a typical solar CME external parts of the asymmetric gaseous envelope of a hot Jupiter located outside its Roche lobe can be torn and carried away into interplanetary medium (Bisikalo & Cherenkov (2016); Cherenkov *et al.* (2017, 2019)). This leads to a sharp increase of the rate of mass loss by a hot Jupiter at the moment when CME passes along it.

As the basis of the numerical model of stellar wind at the time of the passage of CME in the vicinity of the planet, one can take the results of measurements of solar wind parameters at the orbit of the Earth, obtained by space missions ACE, WIND, SOHO in May 1998 during such an event (Farrell *et al.* (2012)). As these measurements show, the process of the passage of CME can be divided into four separate phases. The first phase corresponds to the state of the undisturbed solar wind. The second phase begins with the passage of the front of the MHD-shock and is characterized by an increase of the density n with respect to the unperturbed value n_w by a factor about 4. Velocity v in this case increases 1.3 times with respect to the unperturbed value of v_w. Beyond the front of the shock wave, magnetic field induction B increases 2.25 times with respect to the unperturbed value of B_w. Behind the shock follows the sheath of the heaped matter. The third phase (early CME) begins with the passage of the tangential MHD discontinuity, which propagates following the shock wave. The density drops about two times compared to the unperturbed value. Finally, the fourth phase (late CME) is distinguished by a sharp increase in density (about 10 times relative to the undisturbed wind). However, this phase does not have pronounced limits and, apparently, its beginning is not connected with the passage of any discontinuity. After that, wind parameters return to their original values.

It should be noted that the time profiles of variables in the CME can also have a more general form (Cherenkov *et al.* (2017)). Even for the Sun, intensities of CMEs can greatly vary. For the parent stars of hot Jupiters, these variations may manifest themselves even stronger. A more general approach allows to vary in time the profiles of magnetohydrodynamic quantities, both relative changes of the parameters during the phases and the duration of the phases themselves. In this case, one can describe CMEs of various types, corresponding to slow, medium (Möstl *et al.* (2014)), and fast (Liu *et al.* (2014)) ones.

Let consider now what features of the CME interaction process with the ionospheric envelope of a hot Jupiter may arise, if magnetic field of the stellar wind is taken into account. The influence of the magnetic field can be estimated by the value of the Alfvén Mach number. The changes of the value of the Alfvén Mach number at the different stages of the CME passage can be described by the following expression

$$\frac{\lambda}{\lambda_w} = \sqrt{\frac{n}{n_w}} \frac{v}{v_w} \frac{B_w}{B}. \tag{5.1}$$

As the measurements described by Farrell *et al.* (2012) show, the value of λ varies non-monotonously. In the first phase, λ slightly exceeds the unperturbed value λ_w. In the second phase, λ becomes lower than the unperturbed value λ_w. In the third phase, λ again sharply increases and exceeds unperturbed value λ_w more than three times.

If the planet is deep in the sub-Alfvén zone or, conversely, far in super-Alfvén zone, the nature of the flow during the passage of the CME will not change. In the first case, it will be shockless, as in our calculations presented in Fig. 3. In the second case, entire process, from the beginning to the end, will be accompanied by the formation of detached shock waves, as in our calculations, presented in Fig. 4 and as observed in purely gas-dynamic calculations (Bisikalo & Cherenkov (2016); Cherenkov *et al.* (2017); Kaigorodov

et al. (2019)). However, if the planet's orbit is close to the Alfvén point, the process of interaction of the CME with the magnetosphere may turn out to be more complex and interesting. We recall that for hot Jupiters this should be a very common case (Zhilkin & Bisikalo (2019)).

Let imagine that such a planet is located near the Alfvén point, but at the side of sub-Alfvén zone of the wind. Then, in the second phase, the flow regime should remain shockless, because at this phase the Alfvén Mach number is lower than the unperturbed value λ_w. In the first and third phases, Alfvén Mach number, on the contrary, increases compared to the unperturbed value. Depending on the specific situation, this may be quite enough for the flow velocity to exceed the fast magneto-sonic velocity either in the third phase of the CME or immediately in the first and the third phases. In the first case, in the third phase of the CME a bow shock will emerge, which will disappear again at the end of the entire process and return of the system to the original unperturbed state. In the second case, the shock arises already in the first phase, in the second phase it disappears, then reappears in the third phase and, finally, disappears after passage of CME.

Now, let assume that the hot Jupiter is close to the Alfvén point, but at the side of the super-Alfvén zone of the wind. Then the flow regime can change in the second phase of the CME passage, when the Alfvén Mach number decreases compared to the unperturbed value. That may be quite sufficient to switch the flow into shockless mode, when the flow velocity becomes smaller than the fast magneto-sonic velocity and the bow shock already does not form any more, as in the calculation shown in Fig. 3. As a result of the change in the flow regime bow shock may for some time "switch off" and then "turn on" again after the end of the second phase of the ejection.

6. Conclusion

It is shown in the study that hot Jupiters are located in the sub-Alfvén zone of the stellar wind. However, if the planet's orbital velocity is taken into account, the nature of the flow around the planet approaches the conterminal state separating sub-Alfvén and super-Alfvén regimes. This conclusion was derived using the parameters of the solar wind. Since the parameters of the stellar wind of the parent stars of hot Jupiters can differ significantly from solar wind ones, the corresponding mode of the flow should be investigated separately in each specific case. These results lead to the conclusion that in the studies of the flow of the stellar wind around the atmosphere of a hot Jupiter magnetic field of the wind is an extremely important dynamic factor, which is absolutely necessary to take into account both in theoretical modeling and in the interpretation of observational data.

Magnetospheres of hot Jupiters in the super-Alfvén and sub-Alfvén modes of stellar wind flow around them have significantly different structure. In particular, in the case of the sub-Alfvén regime of the flow around the ionospheric envelope of a hot Jupiter a bow shock wave does not form. In other words, the flow around such a planet is shockless.

The effect of the perturbation of stellar wind parameters, caused by the passage of the coronal mass ejection, upon the nature of the flow near hot Jupiter is considered too. If the orbit of a hot Jupiter is located close to the Alfvén point, the passage of CME may cause temporary formation or disappearance of the shock wave, since the flow can switch from the sub-Alfvén regime to the super-Alfvén one and vice versa. Such phenomena, which significantly change envelope structure, can lead not to the variations in the rate of mass-loss only and, therefore, affect directly the long-term evolution of hot Jupiters, but also affect their observational manifestations.

center Complex for Simulation and Data Processing for Mega-science Facilities at NRC "Kurchatov Institute", http://ckp.nrcki.ru/. This work has been carried out using computational clusters of the Interdepartmental Supercomputer Center of the Russian Academy of Sciences.

References

Arakcheev, A.S., Zhilkin, A.G., Kaigorodov, P.V., *et al.* 2017, *Astronomy Reports*, 61, 932

Ben-Jaffel, L. 2007, *ApJ*, 671, L61

Ben-Jaffel, L., & Sona Hosseini, S. 2010, *ApJ*, 709, 1284

Bisikalo, D.V., Kaigorodov, P.V., Ionov, D.E., & Shematovich, V.I. 2013, *Astronomy Reports*, 57, 715

Bisikalo, D.V., Arakcheev, A.S., & Kaigorodov, P.V. 2017, *Astronomy Reports*, 61, 925

Bisikalo, D.V., Cherenkov, A.A., Shematovich, V.I., *et al.* 2018, *Astronomy Reports*, 62, 648

Bisikalo, D.V., & Cherenkov, A.A. 2016, *Astronomy Reports*, 60, 183

Charbonneau, D., Brown, T.M., Latham, D.W., & Mayor, M. 2000, *ApJ*, 529, L45

Cherenkov, A.A., Bisikalo, D.V., & Kaigorodov, P.V. 2014, *Astronomy Reports*, 58, 679

Cherenkov, A., Bisikalo, D., Fossati, L., Möstl, C. 2017, *ApJ*, 846, 31

Cherenkov, A.A., Bisikalo, D.V., & Kosovichev, A.G. 2018, *MNRAS*, 475, 605

Cherenkov, A.A., Shaikhislamov, I.F., Bisikalo, D.V., *et al.* 2019, *Astronomy Reports*, 63, 94

Farrell, W.M., Halekas, J.S., Killen, R.M., *et al.* 2012, *J. Geophys. Res. (Planets)*, 117, E00K04

Ip, W.-H., Kopp, A., & Hu, J.H. 2004, *ApJ*, 602, L53

Kaigorodov, P.V., Ilyina, E.A., & Bisikalo, D.V. 2019, *Astronomy Reports*, 63, 365

Kislyakova, K.G., Holmström, M., Lammer, H., *et al.* 2014, *Science*, 346, 981

Li, S.-L., Miller, N., Lin, D.N.C., & Fortney, J.J. 2010, *Nature*, 463, 1054

Linsky, J.L., Yang, H., France, K. *et al.* 2010, *ApJ*, 717, 1291

Liu, Y.D., Richardson, J.D., Wang, C., & Luhmann, J.G. 2014, *ApJ*, 788, L28

Mayor, M., & Queloz, D. 1995, *Nature*, 378, 355

Möstl, C., Amla, K., Hall, J.R., *et al.* 2014, *ApJ*, 787, 119

Murray-Clay, R.A., Chiang, E.I., & Murray, N. 2009, *ApJ*, 693, 23

Owens, M.J., & Forsyth, R.J. 2013, *Living Rev. Solar Phys.*, 10, 5

Parker E.N. 1958, *Astrophys. J.*, 128, 664

Roussev, I.I., Gombosi, T.I., Sokolov, I.V., *et al.* 2003, *ApJ*, 595, L57

Russell, C.T. 1993, *Rep. Prog. Phys.*, 56, 687

Steinolfson, R.S., & Hundhausen, A.J. 1988, *J. Geophys. Res.*, 93, 14269

Stevenson, D.J. 1983, *Reports on Progress in Physics*, 46, 555

Totten, T.L., Freeman, J.W., & Arya, S. 1995, *J. Geophys. Res.*, 100, 13

Vidal-Madjar, A., Lecavelier des Etangs, A., Desert, J.-M., *et al.* 2003, *Nature*, 422, 143

Vidal-Madjar, A., Desert, J.-M., Lecavelier des Etangs, *et al.* 2004, *ApJ*, 604, L69

Vidal-Madjar, A., Lecavelier des Etangs, A., Desert, J.-M., *et al.* 2008, *ApJ*, 676, L57

Weber, E.J., & Davis, L., Jr. 1967, *ApJ*, 148, 217

Withbroe, G.L. 1988, *Astrophys. J.*, 325, 442

Zhilkin, A.G., & Bisikalo, D.V. 2019, *Astronomy Reports*, 63, 550

Zhilkin, A.G., Bisikalo, D.V., & Kaygorodov, P.V. 2020, *Astronomy Reports*, in press